

1

Determination of Residual Stresses by Nanoindentation

P-L. Larsson

Department of Solid Mechanics, Royal Institute of Technology, Stockholm, Sweden

1.1 Introduction

Residual stresses and strains in a material can be determined by using various experimental measuring techniques. Examples of such techniques include for example indentation crack techniques [1], fracture-surface analysis, neutron and X-ray tilt techniques [2], beam bending, hole drilling [3], and layer removal [4]. These methods can, however, be both complicated and expensive and therefore, sharp indentation testing, being the method of interest in this chapter, can be a very attractive alternative. It goes almost without saying that this can be of substantial practical importance as the effects of residual stress and strain fields in materials can be considerable with respect to, for example, fatigue, fracture, corrosion, wear, and friction.

Until approximately 20–30 years ago, the influence of residual stresses and residual strains on the results given by a sharp indentation test, in comparison with the corresponding results for a material without residual stresses or residual strains present, i.e. a virgin material, has been studied only occasionally, and then mainly experimentally. This is in contrast to sharp indentation or hardness testing of virgin materials which is a well-known experimental method used for determination of the constitutive properties of conventional materials such as metals and alloys. The method has of course benefitted substantially due to the development of new experimental devices like the nanoindenter (Pethica *et al.* [5]), enabling an experimentalist to determine the material properties from extremely small samples of the material. Indentation testing is for example a very convenient tool for determining the material properties of thin films in ready-to-use engineering devices.

Returning now to the case when residual fields are present, it should be mentioned that already in 1932 Kokubo [6] studied several materials subjected to applied tensile and compressive uniaxial stress. The Vickers hardness was measured and some very small influence from sign and size of the applied stress was found. However, the observed effect of stress on the hardness value was so small that no decisive conclusions could be drawn from these investigations. These results were confirmed somewhat later by Sines and Carlsson [7].

More recently, starting with the study by Doerner and Nix [8], several interesting experimental investigations dealing with this issue were presented, cf. also [9, 10]. The

basic features of the problem were completely understood, however, until Tsui *et al.* [11] and Bolshakov *et al.* [12] investigated, by using nanoindentation as well as numerical methods, the influence of applied stress on hardness, contact area and apparent elastic modulus at indentation of aluminum alloy 8009, an almost elastic-ideally plastic material. Qualitative results of interest were presented as it was shown that the hardness was not significantly affected by applied (residual) stresses while the amount of piling-up of material at the contact contour proved to be sensitive to stress (piling-up increased when the applied stresses were compressive and decreased at tensile stresses).

Based on the results in [11, 12], further studies have been presented, cf. e. g. [13–20], more directed towards the mechanical behavior of the problem. Perhaps being the first to address this issue, Suresh and Giannakopoulos [13] derived, by making certain assumptions on the local stress and deformation fields in the contact region, a relation between the contact area at indentation of a material with elastic residual stresses (and plastic residual strains) and the corresponding contact area at indentation of a material with no stresses present. The analysis in [13] was restricted to equi-biaxial residual stress and strain fields but it should be mentioned that, for the forthcoming discussion, that these authors clearly distinguished between tensile and compressive residual stresses. The relation was, however, approximated with close to linear functions.

The physical understanding of the problem was further developed by Carlsson and Larsson [14, 15], in a combined theoretical, numerical and experimental investigation. A more detailed discussion of the results achieved in [14, 15] will be presented in forthcoming sections below but in short, these authors showed that good correlation between predictions and numerical/experimental results could be achieved if the material yield stress, in relevant indentation parameters, was appropriately replaced by a combination of yield stress and residual stress. Most of the results presented by Carlsson and Larsson [14, 15] were related to equi-biaxial residual stress states but in [15] the derived relations were extended to apply also for more general residual stress fields. In the latter case though, high accuracy results could not be achieved. Furthermore, the accuracy was worse for compressive residual stresses as shown by Larsson [21].

The latter issue was addressed by Rydin and Larsson [20] and very accurate relations linking both compressive and tensile residual stresses to the size of the contact area were presented. Based on the achievements in [20], Larsson [22] attacked the problem pertinent to general residual stresses and presented relations yielding predictions of high accuracy also when neither uniaxial nor equi-biaxial stress state could be assumed.

Below then in the next section, the results presented in [14, 15, 20 and 22] will be explained in detail and it is demonstrated how these findings can be used for determining the residual stresses on the surface of a body. Furthermore, possible improvements of the approach using previous findings concerning the size of the contact area, see e.g. Larsson and Blanchard [23], is discussed as well as the appropriate choice of indenter geometry.

For obvious reasons the presentation here is very much focused on the approach taken by the author. It should be clearly stated though that there are many other research groups, some of them have already been mentioned above, that have suggested alternative approaches yielding promising results. For one thing, another possible approach to the determination of residual stresses by indentation methods is to apply inverse modelling. This has been attempted in a number of studies where perhaps the most general one was presented by Bocciarelli and Maier [19]. These authors used, together with the

standard global indentation properties, the shape of the residual imprint at indentation as a parameter in order to arrive at a unique inverse solution.

Further progress regarding the understanding of the problem concerning residual stresses and indentation was achieved by Huber and Heerens [24] and Heerens *et al.* [25] as these authors analyzed the corresponding problem of residual stress determination using spherical indentation testing. This is a more involved problem (as compared to sharp indentation testing) due to the existence of a characteristic length. Indeed, when elastic and plastic effects are of similar importance self-similarity of the problem is lost and a correlation between the indentation contact pressure and the residual stress state as attempted by Huber and Heerens [24] and Heerens *et al.* [25] becomes very much involved. Despite of this though, also other investigators, see e.g. Swadener *et al.* [26], have suggested that spherical indentation is an attractive approach for residual stress determination. The main reason behind this is that indentation variables are more sensitive to residual stresses in this case (as compared to sharp indentation testing).

Despite the discussion right above, presently sharp indentation is adhered to due to the fact that hardness and relative contact area are independent of indentation depth (due to the fact that the problem is mathematically self-similar with no characteristic length) and this is a particular advantage at interpretation of the results. Furthermore, the emphasis on nanoindentation testing also suggests that sharp indentation is the feature of most interest presently.

1.2 Theoretical Background

The basic foundation of the analysis by Carlsson and Larsson [14, 15], as confirmed by finite element calculations, is that a residual stress field will alter the magnitude but not the principal shape of the field variables involved. This immediately suggests that classical indentation analysis still applies but have to be corrected based on the residual stress. In short, it was shown by Carlsson and Larsson [14, 15] that it is possible to correlate the magnitude of the residual stress field with the well-known Johnson [27, 28] parameter:

$$\Lambda = E \tan \beta / (\sigma_y (1 - \nu^2)) \quad (1.1)$$

In Equation (1), E is the Young's modulus, ν the Poisson's ratio, σ_y the flow stress and β is the angle between the sharp indenter and the undeformed surface of the material, see the (cone) indenter geometry schematically shown in Figure 1.1. Furthermore, in Equation (1.1) elastic-ideally plastic material behavior is assumed.

Johnson [27, 28] suggested that the outcome of a sharp indentation test on an elastic-ideally plastic material falls into one out of three levels, see Figure 1.2, characterized by the parameter Λ in Equation (1.1). In Figure 1.2, H is the material hardness here and in the sequel defined as the average contact pressure. The three levels are schematically shown in Figure 1.2 where in level I, $\Lambda \leq 3$, very little plastic deformation occurs during the indentation test and an elastic analysis of the problem will be sufficient. In level II, $3 < \Lambda < 30$, plastic deformation spreads over the contact area. Finally, in level III, $\Lambda > 30$, pertinent to most engineering metals and alloys, rigid plastic conditions dominate as plastic deformation is present over the entire contact area and elasticity no longer has any effect on the hardness.

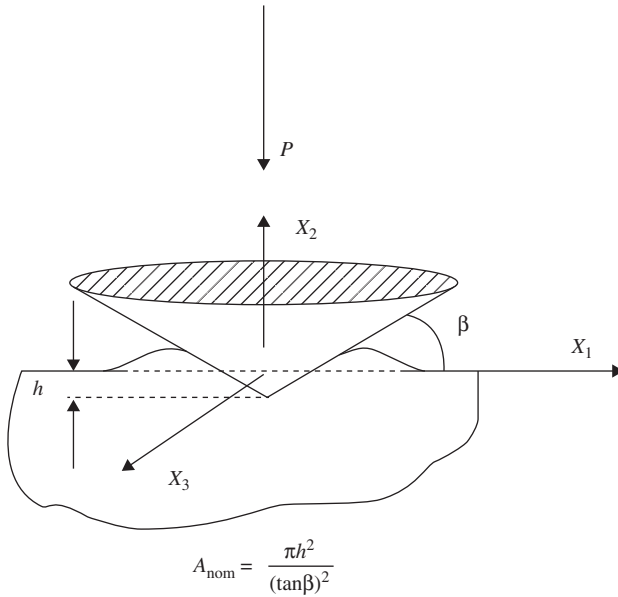


Figure 1.1 Schematic of the geometry of the cone indentation test.

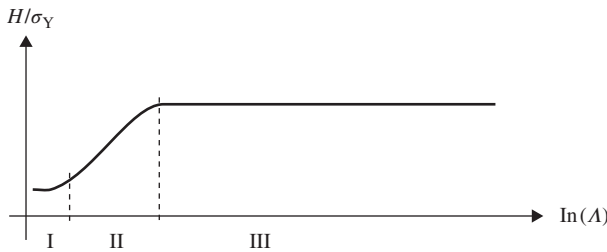


Figure 1.2 Normalized hardness, H/σ_y as a function of $\ln \Lambda$, Λ defined according to Equation (1.1). Schematic of the correlation of sharp indentation testing of elastic-ideally plastic materials as suggested by Johnson [27, 28]. The three levels of indentation responses, I, II and III, are also indicated.

From theoretical, numerical and experimental results [11, 12, 14, 15] it is, as mentioned above, a well-established fact that the material hardness is not noticeably influenced by stresses at sharp indentation testing. The relative contact area, however, here and throughout this chapter defined as:

$$c^2 = A / A_{nom} \tag{1.2}$$

A being the projected true contact area and A_{nom} the nominal contact area as defined in Figure 1.1 for cone indentation, can be directly related to the material state (it should be noted in passing that if $c^2 < 1$ (sinking-in) the resulting contact area is smaller than what could be expected from purely geometrical considerations and the other way around if $c^2 > 1$ (piling-up)). This finding is of fundamental importance when indentation testing is used to determine residual fields and, subsequently, it was shown by Carlsson

and Larsson [14, 15] that when the residual (or applied) stress field is equi-biaxial the relation:

$$c^2 = c^2(\varepsilon_{res}, \sigma_{res} = 0) - 0.32 \ln(1 + (\sigma_{res} / \sigma_y(\varepsilon_{res}))) \quad (1.3)$$

can be expected to give results of high accuracy at tensile stresses but worse at compressive stresses [21]. In Equation (1.3), c^2 is the relative contact area for a material with a (equi-biaxial) residual stress field σ_{res} present (and possibly a (von Mises) effective residual strain field ε_{res}), $c^2(\varepsilon_{res}, \sigma_{res} = 0)$ is the corresponding relative contact area for a material with no residual stress and $\sigma_y(\varepsilon_{res})$ is the material flow stress when the effective plastic strain equal ε_{res} .

In case of ideally-plastic behavior, initially assumed here for simplicity but not necessity, Equation (1.3) reduces to:

$$c^2 = c^2(\sigma_{res} = 0) - 0.32 \ln[1 + (\sigma_{res} / \sigma_y)] \quad (1.4)$$

as then the yield stress of the material is independent of the residual strain field.

Equations (1.3) and (1.4) were derived by Carlsson and Larsson [14, 15] based on the fact that the stress state in the contact region closely resembles the stresses arising at indentation of a virgin material with an initial material yield stress $\sigma_y + \sigma_{res}$. This was shown by careful and comprehensive numerical investigations of the behavior of the indentation induced stress fields as well as deformation fields close to the contact boundary for materials with and without residual stresses.

With this as a background it is then possible to correlate the experimentally determined c^2 -value with the residual stress state based on the universal curve schematically shown in Figure 1.3 by introducing an apparent yield stress:

$$\sigma_{y,apparent} = \sigma_y + \sigma_{res} \quad (1.5)$$

in Λ in Equation (1.1) according to:

$$\Lambda = E \tan \beta / (\sigma_{y,apparent}(1 - \nu^2)) \quad (1.6)$$

The usefulness of this feature rests on the fact that elastic effects are more pronounced for c^2 , than for the material hardness, as also shown in Figure 1.3, and as a result, level II is the dominating region for this parameter.

As mentioned above Equation (1.4) is accurate when a tensile residual stress is at issue but not so at compressive fields. The reason for this is that a compressive residual

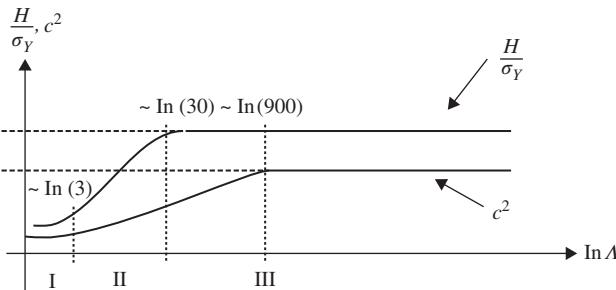


Figure 1.3 Normalized hardness, H / σ_y , and area ratio, c^2 , as functions of $\ln \Lambda$, Λ defined according to Equation (1.1). Schematic of the correlation of sharp indentation testing of elastic-ideally plastic materials. The three levels of indentation responses, I, II and III, are also indicated.

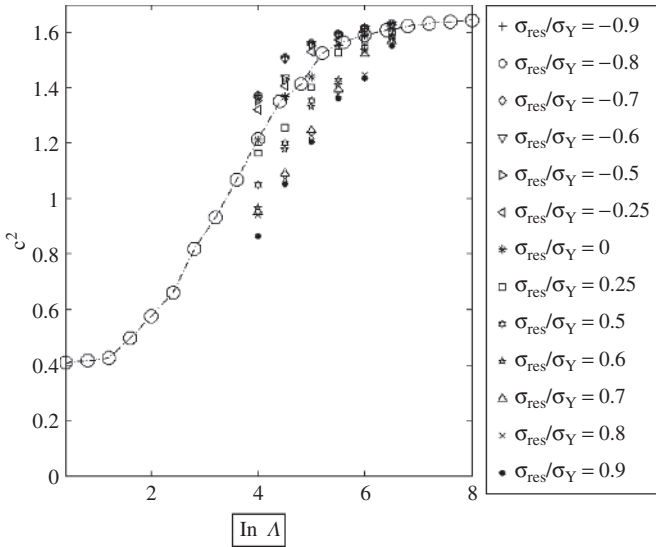


Figure 1.4 The area ratio, c^2 , as function of $\ln \Lambda$, Λ defined according to Equation (1.1). Cone indentation of elastic-ideally plastic materials is considered. *Source:* Rydin 2012 [20]. Reproduced with permission of Elsevier.

stress state will, cf. Equation (1.5), reduce the apparent yield stress $\sigma_{y,apparent}$ leading to a stronger influence from level III indentation effects. This problem was accounted for by Rydin and Larsson [20] (Figures 1.4, 1.5) and in this work it was found, from studying the yield surface at particular points around the contact boundary, that replacing Equation (1.5) with the expression:

$$\sigma_{y,apparent} = \sigma_y + F\sigma_{res}, \tag{1.7}$$

where

$$\begin{aligned} F &= 0.52, \quad \sigma_{res} < 0 \\ F &= 1.77, \quad \sigma_{res} > 0, \end{aligned} \tag{1.8}$$

gave results of very high accuracy both in tension and compression. Explicitly, Rydin and Larsson [20] suggested that the relation:

$$c^2 = c^2(\sigma_{res} = 0) - 0.35 \ln(1 + (F\sigma_{res} / \sigma_y)) \tag{1.9}$$

should replace Equation (1.4) above. It was shown by Rydin and Larsson that Equation (1.9) improved very much on the situation as compared with the results from Equation (1.4). High accuracy predictions in both tension and compression were achieved as depicted in Figures 1.4–1.6 where in particular the excellent agreement in Figure 1.6, pertinent to results based on Equation (1.9), should be noted.

The model by Carlsson and Larsson [14, 15] is based on the fact that the indentation induced in-plane stresses at the contact boundary are compressive and approximately equi-biaxial also when general residual stress states are considered (as shown by extensive finite element calculations). Following the discussion above about the equi-biaxial case, a direct extension would be, as also suggested by Carlsson and Larsson [15], to

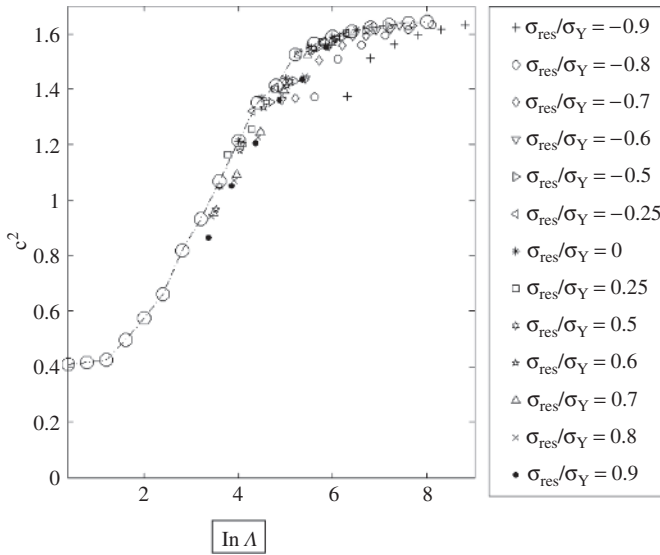


Figure 1.5 The area ratio, c^2 , as function of $\ln \Lambda$, Λ defined according to Equation (1.6) with the yield stress σ_y replaced by the apparent yield stress $\sigma_{y,apparent}$ in Equation (1.5). Cone indentation of elastic-ideally plastic materials is considered. *Source:* Rydin 2012 [20]. Reproduced with permission of Elsevier.

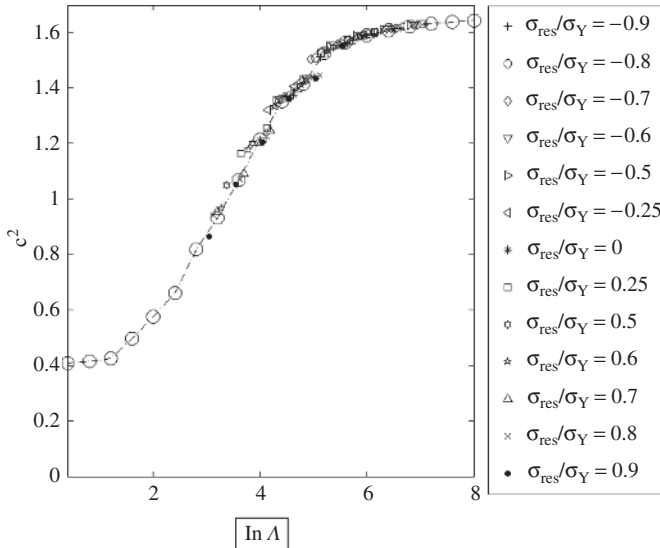


Figure 1.6 The area ratio, c^2 , as function of $\ln \Lambda$, Λ defined according to Equation (1.6) with the yield stress σ_y replaced by the apparent yield stress $\sigma_{y,apparent}$ in Equation (1.7). Cone indentation of elastic-ideally plastic materials is considered. *Source:* Rydin 2012 [20]. Reproduced with permission of Elsevier.

determine the apparent yield stress when an indentation induced compressive and equi-biaxial stress field σ_{ind} is superposed over the surface residual stress field in the material.

The von Mises yield criterion then becomes:

$$\sigma_y^2 = (1/2)((\sigma_1 - \sigma_{yind})^2 + (\sigma_2 - \sigma_{yind})^2 + (\sigma_1 - \sigma_2)^2) \quad (1.10)$$

where σ_{yind} is the apparent yield stress at indentation, $\sigma_{yind} > 0$, while σ_1 and σ_2 are the principal stresses representing the surface residual stress field in the material. The principal stresses are indicated in Figure 1.7 where also the resulting elliptic contact area (at general residual stresses) is shown as defined by the semi-axes a_1 and a_2 .

In the equi-biaxial case the quantity σ_{res} in Equation (1.5) represents the change of the apparent yield stress at indentation. Consequently, it was suggested by Carlsson and Larsson [15] that this quantity could represent also a general residual stress field when determined from the expression:

$$\sigma_{res} = \sigma_{yind} - \sigma_y. \quad (1.11)$$

In Equation (1.11), σ_{yind} is determined from Equation (1.10) and it goes almost without saying that ideally plastic material behavior is assumed.

As already mentioned above, and as also pointed out by Carlsson and Larsson [15], the predictive capability of Equation (1.5), and thereby also Equations (1.10, 1.11), deteriorates substantially at compressive residual stresses. In the equi-biaxial case this was, as also mentioned above, corrected by the results derived by Rydin and Larsson [20] and the basic results in [20] were used by Larsson [22] in order to determine prediction also in a general case. Explicitly then in [22], the relation between the relative contact area c^2 and the residual stress state σ_{res} , determined from Equations (1.10) and (1.11), were

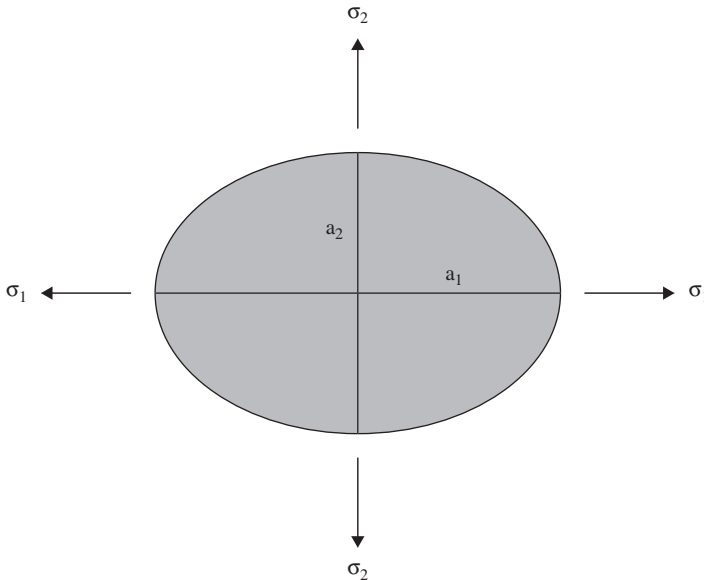


Figure 1.7 Schematic of the contact area (shaded) at indentation. The principal residual stresses and the corresponding semi-axes of the elliptical contact area are also indicated.

expressed by Equation (1.9) also generally. In short, Larsson [22] reported high accuracy predictions based on this approach. In this context it should be clearly stated that the nature of the stress state, based on the ratio σ_1/σ_2 , enters the analysis by Larsson [22] through σ_{res} . However, it is only possible to derive the magnitude of the residual stresses involved based on such approach and in order to also determine explicit values on the ratio σ_1/σ_2 additional experimental information is needed. Such information can, as suggested in [22], be given from the elliptic shape of the contact area, see Figure 1.7, i.e. the value on the ratio a_1/a_2 .

It was shown, however, by Larsson and Blanchard [23] that even though such an approach is possible (the influence from the ratio σ_1/σ_2 on a_1/a_2 can be proven) such influence is very weak in case of cone indentation and will not be of practical use in an experimental situation. A more complex indenter geometry would then be advantageable and possibly a Knoop indenter should be relied upon for this purpose remembering the rhombic shape of this indenter. This issue, however, remains to be investigated.

The relations presented are, as already stated above, pertinent to elastic-ideally plastic behavior. In order to extend the validity of the present approach to strain-hardening materials, it is possible to draw upon results from a previous study by Larsson [29]. In this study it is assumed that the indented material is well described by a power law material with a uniaxial stress-strain relation according to:

$$\sigma(\varepsilon_p) = \sigma_y + \sigma_0(\varepsilon_p)^{1/n}, \quad (1.12)$$

where σ_0 and n are material constants and ε_p is the accumulated effective plastic strain. It was then shown that at level II cone indentation the nominal contact area could always be expressed as:

$$c^2 = C_1(n) + C_2(n) \ln(\Lambda_h) \quad (1.13)$$

with

$$C_1(n) = -0.07 + 0.75(1/n) - 0.29(1/n)^2 \quad (1.14)$$

and

$$C_2(n) = 0.30 - 0.29(1/n) + 0.09(1/n)^2 \quad (1.15)$$

Derived from curve-fitting based on the results by Larsson [29]. In Equation (1.13) Λ_h is the Johnson's parameter [27, 28] in Equation (1.1) also accounting for strain-hardening according to:

$$\Lambda_h = E \tan \beta / [\sigma_r(1 - \nu^2)] \quad (1.16)$$

where σ_r is a stress measure representing in an average sense the plastic strain-hardening of the indented material. Traditionally, the suggestion by Tabor [30] (where σ_r is the flow stress at $\varepsilon_p = 0.08$) is used but it was shown by Larsson [31] that the choice:

$$\sigma_r = 0.392\sigma(\varepsilon_p = 0.02) + 0.608\sigma(\varepsilon_p = 0.35) \quad (1.17)$$

yields better accuracy in a general situation. It should be noted in passing that the actual values on the constants in Equations (1.13, 1.14, 1.15 and 1.17) are pertinent to cone indentation with an angle $\beta = 22^\circ$, see Figure 1.1. These constants will change in case of

Vickers and Berkovic indentation, the latter being more pertinent to nanoindentation, as discussed in detail in [31].

Returning to Equation (1.13) and recalling that the constant $C_2(n)$ determines the slope of the Johnson-curve [27, 28] in a situation where strain-hardening effects are present. It is then straightforward, when strictly following the reasoning above leading to Equation (1.3) and (1.9), to derive the relation:

$$c^2 = c^2(\sigma_{res} = 0) - C_2(n) \ln(1 + (F\sigma_{res} / \sigma_r)) \quad (1.18)$$

In (16) it has been tentatively assumed that the apparent representative stress is changed due to a residual stress state σ_{res} based on Equation (1.10) according to:

$$\sigma_{r,apparent} = \sigma_r + F\sigma_{res}, \quad (1.19)$$

see Equation (1.7), and that any (von Mises) effective residual strain ϵ_{res} can be neglected. In this context it should be immediately emphasized that it remains to determine the validity of Equations (1.18) and (1.19) as, for one thing, the variation of F at plastic strain-hardening is not known.

In summary then, from the discussion above it is hopefully clear that the basic theoretical foundation exists for accurate determination of residual stress field by nanoindentation. In particular when it comes to equi-biaxial residual stresses in low hardening materials, a full theory is available. This is also the case to be discussed in detail below in the context of practical applications. However, concerning the effects from plastic strain-hardening and general biaxiality a complete theory is not yet, as also discussed above, available even though the relations (1.10, 1.11, 1.18 and 1.19) are of direct relevance for at least qualitative predictions. These issues will also be discussed further.

1.3 Determination of Residual Stresses

As just mentioned above, in this section a solution strategy for the determination of residual stresses by indentation will be discussed and outlined in the context of the theory presented above. The solution strategy will mainly concentrate on equi-biaxial residual stresses in low hardening materials but also a general approach is discussed. In most cases, no distinction is made between standard indentation and nanoindentation but when so required, this will be specified.

1.3.1 Low Hardening Materials and Equi-biaxial Stresses

What is considered then first is a low hardening material accurately described by classical Mises plasticity. It is assumed that the material constants at issue are known from experiments on a virgin material (a material with no residual stresses or strains present). Furthermore, it is also assumed that the hardness, $H(\sigma_{res} = 0)$, and relative contact area, $c^2(\sigma_{res} = 0)$, of the virgin material is known from previous experiments.

Accordingly, the first step in the procedure concerns the determination of the virgin properties $H(\sigma_{res} = 0)$, and $c^2(\sigma_{res} = 0)$. It should be immediately emphasized that these properties are independent of any residual strain fields present due to the fact that only ideal plasticity (or close to ideal plasticity) is considered. This, however, will be discussed in some more detail below.

Furthermore in this context and in the context of particular issues related to nanoindentation, it is important to emphasize that when determining indentation properties the contact area should always be determined from optical measurements. As a standard procedure at nanoindentation, the contact area is determined from the indentation load–indentation depth (P - h) relation according to the procedure suggested by Oliver and Pharr [32]. However, such an approach can give results of low accuracy leading to erroneous conclusions as shown by Bolshakov *et al.* [12].

In the next step the surface of the material with residual stresses is indented and the hardness, $H(\sigma_{res})$, and the relative contact area, $c^2(\sigma_{res})$, are determined. The reason for recording also the hardness values, $H(\sigma_{res} = 0)$, and $H(\sigma_{res})$, is as mentioned above to check the invariance of hardness at ideal plasticity (or close to ideal plasticity). The two simple steps so described, nanoindentation of the material in a virgin and in a stressed state, constitute (together with the material characterization of the virgin material) the experimental part of the procedure aiming at residual stress determination.

The third and final step in this procedure concerns explicit determination of the equi-biaxial residual surface stress σ_{res} from Equation (1.9). Remembering that both $c^2(\sigma_{res} = 0)$ and $c^2(\sigma_{res} = 0)$, as well as the material yield stress σ_y , are known from the introductory experiments it is then a straightforward task to calculate σ_{res} (as σ_{res} is the only unknown in Equation (1.9)). The only consideration that has to be made is the explicit value on the constant F in Equation (1.9). In short, if $c^2(\sigma_{res}) > c^2(\sigma_{res} = 0)$ this implies that the residual stress state is compressive and, consequently, if $c^2(\sigma_{res}) < c^2(\sigma_{res} = 0)$ tensile residual stresses are present on the surface of the material. Based on the sign of σ_{res} , the value on F can be determined in a straightforward manner according to Equation (1.8).

Clearly, in the case of low hardening materials and equi-biaxial stresses it is at least in theory a rather straightforward task using the present approach to determine the relevant variables describing the residual stress field. However, if these restrictions do not apply, the situation becomes much more difficult and indeed, for some particular cases additional research is needed as outlined above.

1.3.2 General Residual Stresses

One of the complicating issues concerns the case when equi-biaxiality cannot be assumed. However, as mentioned above a solution approach for this case has been suggested by Larsson [22], based on Equations (1.10 and 1.11) together with Equation (1.9), yielding high accuracy predictions in a situation when the explicit value on the ratio between the residual stresses, σ_1 / σ_2 , is known, for example in a uniaxial situation, see Figure 1.8 pertinent to an ideally-plastic material. If this ratio is not known, however, further information is needed for a complete determination of the residual stresses in the material.

An obvious candidate to provide such additional information would of course possibly be given from the elliptic shape of the contact area, see Figure 1.7, i. e. the value on the ratio a_1 / a_2 . However, as mentioned above, it was shown by Larsson and Blanchard [23] that even though such an approach is possible this influence from the ratio σ_1 / σ_2 on a_1 / a_2 is very weak in case of cone indentation, cf. e. g. results by Larsson and Blanchard [23, 33] as shown in Figures 1.9 and 1.10 for two different values on the Johnson [27, 28] parameter Λ , and most likely also for other highly symmetric indenters such as the

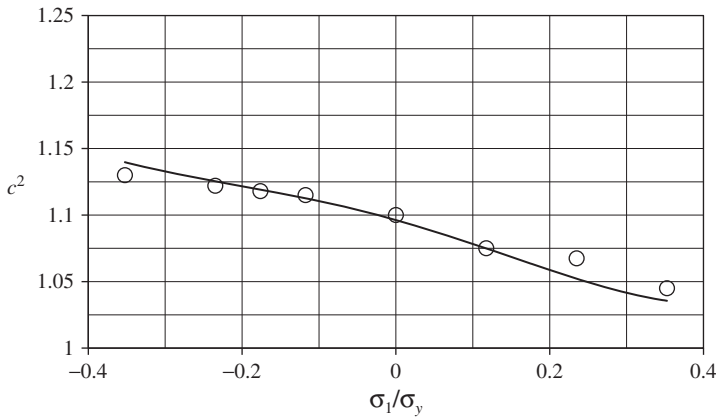


Figure 1.8 Berkovich indentation of an aluminum alloy 8009 ($E = 82.1$ GPa, $\nu = 0.31$, $\sigma_y = 425.6$ MPa (this is the peak stress after a small amount of initial work-hardening), $c^2(\sigma_{res} = 0) = 1.10$). The area ratio c^2 is shown as function of an applied uniaxial stress (ratio) σ_1/σ_y . (O), experimental results by Tsui *et al.* [11]. (—), theoretical predictions by Larsson [22]. *Source:* Larsson 2014. Reproduced with permission of Springer.

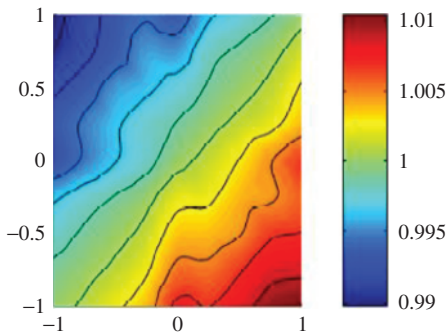


Figure 1.9 Semi-axes ratio a_1/a_2 , see Figure 1.7, as function of the principal stress ratios σ_1/σ_y (horizontal axis) and σ_2/σ_y (vertical axis). Explicit values on a_1/a_2 are determined by the colors on the right hand side of the figure. The value on the Johnson [27, 28] parameter is $\Lambda = 100$. *Source:* Larsson 2012 [23]. Reproduced with permission of Elsevier.

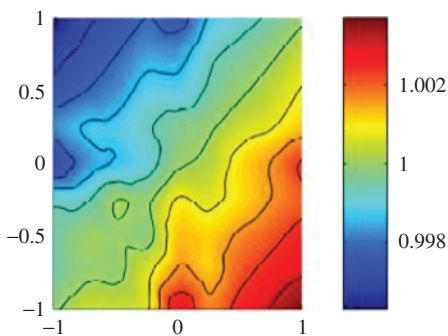


Figure 1.10 Semi-axes ratio a_1/a_2 , see Figure 1.7, as function of the principal stress ratios σ_1/σ_y (horizontal axis) and σ_2/σ_y (vertical axis). Explicit values on a_1/a_2 are determined by the colors on the right hand side of the figure. The value on the Johnson [27, 28] parameter is $\Lambda = 300$. *Source:* Larsson 2012 [23]. Reproduced with permission of Elsevier.

Vickers and the Berkovic indenters. As mentioned previously the Knoop indenter could then be a possible choice of indenter in order to improve the influence on a_1/a_2 from the stress ratio σ_1/σ_2 . This is definitely an important future research direction which, at least when numeric analysis is concerned, would not introduce any fundamental difficulties as finite element analyses of sharp indentation is now very much a standard task, cf. [34–38] for early efforts. Indeed, such analysis have been conducted previously, [39–41], but not in the context of determination of residual stresses.

1.3.3 Strain-hardening Effects

Further complications related to the theory outlined above concerns plastic strain-hardening effects. In this context, Carlsson and Larsson [14, 15] used Equation (1.3) for this feature primarily in the equi-biaxial case. It should then be noticed that the information needed in this case are not only the quantities $H(\varepsilon_{res}, \sigma_{res})$ $c^2(\varepsilon_{res}, \sigma_{res})$, for the stressed material, but also the stress-free quantities $H(\varepsilon_{res}, \sigma_{res} = 0)$ and $c^2(\varepsilon_{res}, \sigma_{res} = 0)$ where ε_{res} represents, as indicated above, the influence from residual plastic deformation due to plastic strain-hardening on the global indentation properties.

It is to be expected that the hardness values are independent of any residual stresses, cf. [12] and [14], but this quantity should be used to determine ε_{res} from the original uniaxial stress–strain curve via an appropriate relation between hardness and plastic strain hardening, cf. Tabor [30] and Larsson [31].

If equi-biaxiality can be assumed it is then a straightforward matter, based on the experimental information achieved, to determine the residual stress σ_{res} via Equations (1.18 and 1.19) where of course also (if necessary) a residual field ε_{res} can be accounted for in Equation (1.18) according to:

$$c^2(\varepsilon_{res}, \sigma_{res}) = c^2(\varepsilon_{res}, \sigma_{res} = 0) - C_2(n) \ln(1 + (F\sigma_{res}/\sigma_r)) \quad (1.20)$$

as discussed just above. As stated previously, it remains, however, to determine the validity of Equations (1.18 and 1.19), and of course Equation (1.20) as, for one thing, the variation of F at plastic strain-hardening is not known.

Finally, in this context, it should also be mentioned that when equi-biaxiality is lost at strain-hardening plasticity the situation becomes even more involved. In theory, Equations (1.10 and 1.11), together with Equation (1.20), could be applied as in the corresponding ideally-plastic case but again, the validity of such an approach needs to be investigated in more detail. Clearly, again as in the ideally-plastic case, further information is needed for a complete determination of the residual stresses.

1.3.4 Conclusions and Remarks

It should be emphasized that the discussion above is essentially restricted to cone indentation. However, as shown by Carlsson and Larsson [15], basically the same solution strategy could be applied to pyramid indenter geometries such as the Vickers and Berkovich indenters, the latter being more pertinent to nanoindentation, even though the details might be different. This issue concerns for example the definition of the representative stress in Equation (1.17), as discussed in detail by Larsson [31], where for pyramid indenters this relation yields:

$$\sigma_r = 0.5(\sigma(\varepsilon_p = 0.02) + \sigma(\varepsilon_p = 0.35)). \quad (1.21)$$

Finally, it is worth mentioning that the present approach could very well be applied to other types of contact problems as well. One of these problems could be scratching and scratch testing where correlation of material and contact properties, in the spirit of Johnson [27, 28], have been discussed for some time now, cf. [42–51]. It remains, however, to undertake an analysis that incorporates also residual stresses in this type of correlation.

References

- 1 Marshall DB, Lawn BR. Indentation of brittle materials. ASTM Special Technical Publications 889, 26–46; 1985.
- 2 Hehn L, Zheng C, Mecholsky JJ, Hubbard CR. Measurements of residual-stresses in Al₂O₃/Ni laminated composites using an X-ray-diffraction technique. *Journal of Materials Science* 30, 1277–1282; 1995.
- 3 Rendler N.J, Vigness I. Hole-drilling strain-gauge method of measuring residual stresses. *Experimental Mechanics* 13, 45–48; 1973.
- 4 Flavenot JF, Nikulari A. Mesures des contraintes résiduelles, method de la fleche. *Les Memories Technique du Cetim* 31, 6–42; 1977.
- 5 Pethica JB, Hutchings R, Oliver WC. Hardness measurements at penetration depths as small as 20 nm. *Philosophical Magazine* A48, 593–606; 1983.
- 6 Kokubo, S. On the change in hardness of a plate caused by bending. *Science Reports of the Tohuko Imperial University ser.1*, 21, 256–267; 1932.
- 7 Sines G, Carlson R. Hardness measurements for determination of residual stresses. *ASTM Bulletin* 180, 357; 1952.
- 8 Doerner MF, Gardner DS, Nix WD. Plastic properties of thin films on substrates as measured by submicron indentation hardness and substrate curvature techniques. *Journal of Materials Research* 1, 845–851; 1986.
- 9 LaFontaine WR, Yost B, Li CY. Effect of residual stress and adhesion on the hardness of copper films deposited on silicon. *Journal of Materials Research* 5, 776–783 (1990).
- 10 LaFontaine WR, Paszkiet CA, Korhonen MA, Li CY. Residual stress measurements of thin aluminum metallizations by continuous indentation and X-ray stress measurement techniques. *Journal of Materials Research* 6, 2084–2090; 1991.
- 11 Tsui TY, Oliver WC, Pharr GM. Influences of stress on the measurement of mechanical properties using nanoindentation. Part I. Experimental studies in an aluminum alloy. *Journal of Materials Research* 11, 752–759; 1996.
- 12 Bolshakov A, Oliver WC, Pharr GM. Influences of stress on the measurement of mechanical properties using nanoindentation. Part II. Finite element simulations. *Journal of Materials Research* 11, 760–768; 1996.
- 13 Suresh S, Giannakopoulos AE. A new method for estimating residual stresses by instrumented sharp indentation. *Acta Materialia* 46, 5755–5767; 1998.
- 14 Carlsson S, Larsson PL. On the determination of residual stress and strain fields by sharp indentation testing. Part I. Theoretical and numerical analysis. *Acta Materialia* 49, 2179–2191; 2001.

- 15 Carlsson S, Larsson PL. On the determination of residual stress and strain fields by sharp indentation testing. Part II. Experimental investigation. *Acta Materialia* 49, 2193–2203; 2001.
- 16 Lee YH, Kwon D. Measurement of residual-stress effect by nanoindentation on elastically strained (100)W. *Scripta Materialia* 49, 459–465; 2003.
- 17 Lee YH, Kwon D. Stress measurement of SS400 steel beam using the continuous indentation technique. *Experimental Mechanics* 44, 55–61; 2004.
- 18 Lee YH, Kwon D. Estimation of biaxial surface stress by instrumented indentation with sharp indenters. *Acta Materialia* 52, 1555–1563; 2004.
- 19 Bocciarelli M, Maier G. Indentation and imprint mapping method for identification of residual stresses. *Computational Materials Science* 39, 381–392; 2007.
- 20 Rydin A, Larsson PL. On the correlation between residual stresses and global indentation quantities: Equi-biaxial stress field. *Tribology Letters* 47, 31–42; 2012.
- 21 Larsson PL. On the mechanical behavior at sharp indentation of materials with compressive residual stresses. *Mater Design* 32, 1427–1434; 2011.
- 22 Larsson PL. On the determination of biaxial residual stress fields from global indentation quantities. *Tribol Lett* 54, 89–97; 2014.
- 23 Larsson PL, Blanchard P. On the correlation between residual stresses and global indentation quantities: Numerical results for general biaxial stress fields. *Materials Design* 37, 435–442; 2012.
- 24 Huber N, Heerens J. On the effect of a general residual stress state on indentation and hardness testing. *Acta Materialia* 56, 6205–6213; 2008.
- 25 Heerens J, Mubarak F, Huber N. Influence of specimen preparation, microstructure anisotropy, and residual stresses on stress-strain curves of rolled Al2024 T351 as derived from spherical indentation tests. *Journal of Materials Research* 24, 907–917; 2009.
- 26 Swadener JG, Taljat B, Pharr GM. Measurement of residual stress by load and depth sensing indentation with spherical indenters. *Journal of Materials Research* 16, 2091–2102; 2001.
- 27 Johnson, K.L.: The correlation of indentation experiments. *Journal of the Mechanics and Physics of Solids* 18, 115–126; 1970.
- 28 Johnson KL. *Contact Mechanics*. Cambridge University Press, Cambridge; 1985.
- 29 Larsson PL. On the mechanical behavior of global parameters in material characterization by sharp indentation testing. *Journal of Testing and Evaluation* 32, 310–321; 2004.
- 30 Tabor D.: *Hardness of Metals*. Cambridge: Cambridge University Press, Cambridge; 1951.
- 31 Larsson PL. Investigation of sharp contact at rigid plastic conditions. *International Journal of Mechanical Science* 43, 895–920; 2001.
- 32 Oliver WC, Pharr GM. An improved technique for determining hardness and elastic modulus using load and displacement sensing indentation experiments. *Journal of Materials Research* 7, 1564–1583; 1992.
- 33 Larsson PL, Blanchard P. On the invariance of hardness at sharp indentation of materials with general biaxial residual stress fields. *Materials Design* 52, 602–608; 2013.
- 34 Bhattacharya AK, Nix WD. Finite-element simulation of indentation experiments. *International Journal of Solids and Structures* 24, 881–891; 1988.

- 35 Bhattacharya AK, Nix WD. Analysis of elastic and plastic deformation associated with indentation testing of thin films on substrates. *International Journal of Solids and Structures* 24, 1287–1298; 1988.
- 36 Laursen TA, Simo JC. A study of the mechanics of microindentation using finite-elements. *Journal of Materials Research* 7, 618–626; 1992.
- 37 Giannakopoulos AE, Larsson PL, Vestergaard R. Analysis of Vickers indentation. *International Journal of Solids and Structures* 31, 2679–2708; 1994.
- 38 Larsson PL, Söderlund E, Giannakopoulos AE, *et al.* Analysis of Berkovich indentation. *International Journal of Solids and Structures* 33, 221–248; 1996.
- 39 Giannakopoulos AE, Zisis T. Analysis of Knoop indentation. *International Journal of Solids and Structures* 48, 175–190; 2011.
- 40 Zisis T, Giannakopoulos AE. Analysis of Knoop indentation strain hardening effects. *International Journal of Solids and Structures*, 48, 3217–3231; 2011.
- 41 Giannakopoulos AE, Zisis T. Analysis of Knoop indentation of cohesive frictional materials. *Mechanics of Materials* 57, 53–74; 2013.
- 42 Bucaille JL, Felder E, Hochstetter G. Mechanical analysis of the scratch test on elastic and perfectly plastic materials with three-dimensional finite element modeling. *Wear* 249, 422–432; 2001.
- 43 Bucaille JL, Felder E, Hochstetter G. Experimental and three-dimensional finite element study of scratch test of polymers at large deformations. *Journal of Tribology* 126, 372–379; 2004.
- 44 Felder E, Bucaille JL. Mechanical analysis of the scratching of metals and polymers with conical indenters at moderate and large strains. *Tribology International* 39, 70–87; 2006.
- 45 Bellemare S, Dao M, Suresh S. The frictional sliding response of elasto-plastic materials in contact with a conical indenter. *International Journal of Solids and Structures* 44, 1970–1989; 2007.
- 46 Wredenberg F, Larsson PL. On the numerics and correlation of scratch testing. *Journal of the Mechanics of Materials and Structures* 2, 573–594; 2007.
- 47 Ben Tkaya M, Zidi M, Mezlini S, *et al.* Influence of the attack angle on the scratch testing of an aluminium alloy by cones: Experimental and numerical studies. *Materials Design* 29, 98–104; 2008.
- 48 Wredenberg F, Larsson PL. Scratch testing of metals and polymers—experiments and numerics. *Wear* 266, 76–83; 2009.
- 49 Aleksey N, Kermouche G, Vautrin A, Bergheau JM. Numerical study of scratch velocity effect on recovery of viscoelastic-viscoplastic solids. *International Journal of Mechanical Sciences* 52, 455–463; 2010.
- 50 Bellemare S, Dao M, Suresh S. A new method for evaluating the plastic properties of materials through instrumented frictional sliding tests. *Acta Materialia* 58, 6385–6392; 2010.
- 51 Larsson PL. On the correlation of scratch testing using separated elastoplastic and rigid plastic descriptions of the representative stress. *Materials Design* 43, 153–160; 2013.